JACS
JOURNAL OF THE AMERICAN CHEMICAL SOCIETY
Article
pubs.acs.org/JACS

Small-Molecule-Triggered and Light-Controlled Reversible Regulation of Enzymatic Activity

Tian Tian,[†,‡] Yanyan Song,[†,‡] Jiaqi Wang,[†] Boshi Fu,[†] Zhiyong He,[†] Xianqun Xu,[§] Anling Li,[§] Xin Zhou,[§] Shaoru Wang,[*,†] and Xiang Zhou[*,†]

[†]College of Chemistry and Molecular Sciences, Institute of Advanced Studies, Key Laboratory of Biomedical Polymers of Ministry of Education, Wuhan University, Wuhan 430072, Hubei Province, China

[§]Zhongnan Hospital, Wuhan University, Wuhan 430071, Hubei Province, China

Supporting Information

ABSTRACT: The fine control of enzyme activity is essential for the regulation of many important cellular and organismal functions. The light-regulation of proteins serves as an important method for the spatiotemporal control over the production and degradation of an enzyme product. This area is of intense interest for researchers. To the best of our knowledge, the use of small molecules as light-triggered molecular switches to reversibly control enzyme activity at the protein level has not yet been studied. In the present study, we demonstrate the light-controlled reversible regulation of the enzyme using a small-molecule-triggered switch, which is based on molecular recognition between an azobenzene derivative and telomere DNA. This molecule interconverts between the *trans* and *cis* states under alternate 365 nm UV and visible light irradiation, which consequently triggers the compaction and extension of telomere DNA. We further provide direct evidence for this structural switch using a circular dichroism study. Furthermore, our strategy has been successfully used to effectively control blood clotting in human plasma.

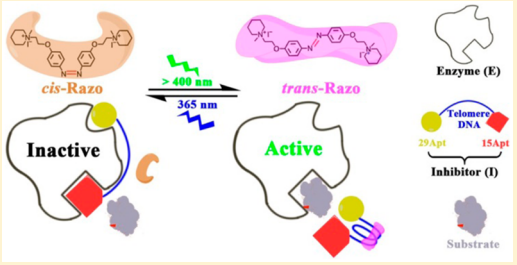

INTRODUCTION

The reversible regulation of the cellular enzymes can have profound importance in biology, and this area has garnered intense interest.[1,2] Many enzymes are controlled by changes in their structure or conformation, which consequently determine their catalytic activity.[3] These conformational changes may result from the binding/dissociation of different effectors or regulators.[4,5] In recent studies, scientists have identified important molecules with regulatory functions.[6−8] For example, aptamers have been generated by in vitro selection.[9,10] They are oligonucleotide molecules that can specifically bind to their targets with a high affinity.[11−14] Therefore, they have been used to control enzymatic activities.[15]

Light is an external stimulus and provides a very convenient way to manipulate various objects at a desired time and in a desired area.[16−19] Recently, significant progress has been made in developing nucleic acid-based photocontrollers.[20,21] For example, photoactivatable oligonucleotides have been developed by attaching photolabile groups.[22−24] Although functional oligonucleotides can be efficiently generated by irradiating caging groups,[25] this regulating process is usually irreversible. Some chemical moieties, such as azobenzene chromophores,[26,27] possess excellent photoresponsive merits and have consequently been developed as reversible photoswitchable tools.[28−30] Strikingly, DNA hybridization,[31] replication[32] and transcription[33] have been regulated using azobenzene-tethered DNAs. Due to their high specificity and ease of use, azobenzene modified aptamers have been used in a wide range of fields, such as chemical sensors and nanomachines.[34]

As mentioned above, these known studies usually depend on photochromic oligonucleotides.[35,36] Unfortunately, the synthesis of modified oligonucleotides poses outstanding challenges for researchers due to their large size and complexity. More recently, the development of DNA nanotechnology has offered a powerful route to dynamically control enzymes.[37,38] Several key studies demonstrate that the binding affinity of aptamers to the target can be significantly improved by proximity-dependent surface hybridization.[39−42] Moreover, the protein activity has been successfully modulated by adjusting closed-loop structures.[43] However, the manipulation of these strucures is a relatively complex process that must be strictly controlled. Photocontrollers based on small molecules are of great interest because they are both cheaper to make and easier to process than those based on modified macromolecules. A photosensitive DNA binder can reportedly regulate gene expression in a reversible and sequence-independent manner.[44] Therefore, we attempted to control enzymes using small-molecule triggers.

Under different conditions, nucleic acids can form various secondary structures via complex hydrogen bonds.[45] G-quadruplexes are four-stranded DNA structures and can be regulated by small molecules.[46] Recently, we first studied the

Received: November 9, 2015
Published: January 7, 2016

DOI: 10.1021/jacs.5b11532
J. Am. Chem. Soc. 2016, 138, 955−961

properties of Razo (structure in Figure S1), which is an azobenzene derivative.[47] Remarkably, this molecule isomerizes between *trans* and *cis* states under ultraviolet (UV) ↔ visible light (VIS) illumination. More importantly, our previous findings clearly demonstrated that it is able to reversibly control the conformations of telomere DNA upon photoirradiation.[47] Therefore, this small-molecule-triggered photoregulation of DNA conformation can be potentially used to control enzymes.

In the current study, we have developed an EIR system that contains three dependent components as follows: enzyme (E), inhibitor (I) and the azobenzene derivative Razo (R). Using this system, we demonstrate the light-triggered reversible control of an enzyme via a small-molecule switch (Figure 1).

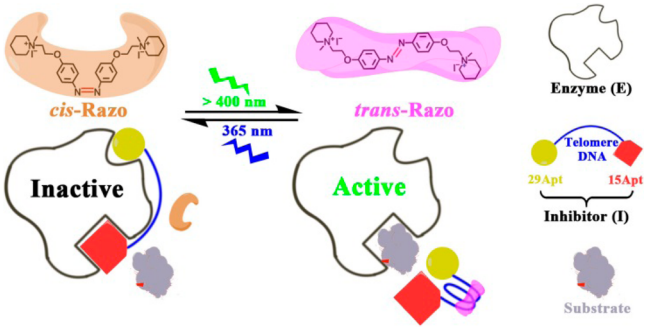

Figure 1. Schematic illustration of small-molecule-triggered and light-controlled reversible regulation.

This switch is based on molecular recognition between Razo and telomere DNA. Razo interconverts between the *trans* and *cis* states under alternate 365 nm UV and VIS (>400 nm) irradiation, which consequently triggers the compaction or extension of the DNA-based inhibitor. We further provide direct evidence for this structural switch through a circular dichroism (CD) study. Furthermore, our strategy has been successfully used to modulate the clotting process of human plasma.

RESULTS AND DISCUSSION

Design of Small-Molecule-Triggered Light Controller.

In the current study, we attempted to regulate enzymes using a small-molecule-triggered light controller. To demonstrate the proof-of-concept of our strategy, the thrombin-fibrinogen reaction is used as the model system. Thrombin is a valuable biochemical tool due to its high proteolytic specificity.[48] Moreover, it plays a significant role in thrombosis and hemostasis.[49] As the substrate for thrombin, fibrinogen is a soluble plasma glycoprotein and can be converted into insoluble fibrin fibers.[50] Dynamic light scattering is commonly used to investigate the dynamics of this process, and the enhancement of light scattering intensity (LSI) represents the progress of this reaction.[2,43]

A key part of our working principle will be the rational design of the DNA-based inhibitor. For our purpose, human telomere DNA with the sequence of $dG_3(T_2AG_3)_3$ was fused into the middle region of this inhibitor. As the regulatory linker, it was allowed to change conformations (being flexible) through interactions with *cis*-Razo or *trans*-Razo. In addition, the inhibitor contains two binding partners that cooperatively prevent the binding of fibrinogen. Two thrombin binding aptamers (15Apt and 29Apt) are used as the binding partners.[9,10] 15Apt is located near the 5′ end, while 29Apt is at the 3′ end. Therefore, the inhibitor Itelo (sequence in Table S1) was designed and it was expected to be reversibly switched between the two distinct states. *trans*-Razo induces and binds exclusively to Itelo in its compact state (possible G4 structure), while *cis*-Razo does not bind to Itelo in its extended state.

Regulating Thrombin upon Photoirradiation of Razo.

Razo is synthesized according to a previously reported procedure.[47] We first studied the influence of Razo on thrombin. Human thrombin was treated with various concentrations of Razo in the absence of Itelo. Our results indicate that Razo itself does not significantly affect thrombin (Figure S2). Even when thrombin was treated with a high concentraion (40 μM) of Razo, the LSI increased at a rate comparable to that observed for untreated thrombin. We next investigated whether Itelo can inhibit thrombin in the absence of Razo. Therefore, thrombin was treated with different concentrations of Itelo. Not surprisingly, this inhibitor works very well. Thrombin was evidently inhibited by 0.5 nM Itelo, and 2.0 nM Itelo resulted in complete inhibition (Figure S3). These findings are the first step toward the success of our strategy.

On the basis of a previous study,[47] the newly synthesized Razo is predominantly in the *trans* conformation, and the population of this conformation tends to induce and bind to the compact telomere DNA. This specific folding event thus brings 15Apt and 29Apt into close proximity; in other words, they cannot bind together to thrombin (Figure S4). Thrombin will therefore be activated. To test this mechanism, thrombin was completely preinactivated by Itelo, and various amounts of *trans*-Razo were then added to this solution. This solution was then incubated further to generate the three-component *trans*-EIR system (Figure S4). Figure 2 shows representative data for

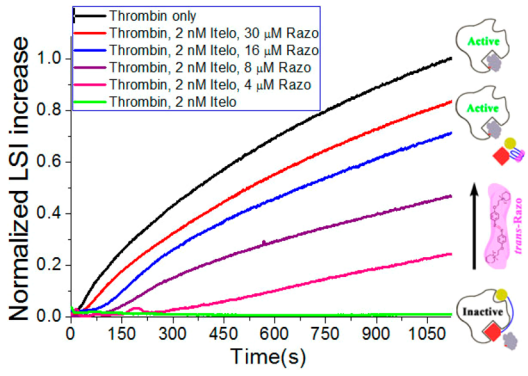

Figure 2. Razo recovers thrombin from inactivation. The newly synthesized Razo (in the *trans* conformation) was used here. Human thrombin (0.10 U/mL) was inactivated by the inhibitor Itelo (2.0 nM) and then treated with various concentrations of Razo ranging from 0 μM (control) to 30 μM. The LSI of the sample versus time is shown. The LSI increase of the sample was normalized to that of the control sample (thrombin only), and this increase directly correlated with the amount of Razo present in the sample.

the LSI increase of the sample as a function of time. In agreement with our expectation, *trans*-Razo recovered the activities of thrombin in a dose-dependent manner. Specifically, 4.0 μM *trans*-Razo treatment allowed a proportion of thrombin to recover from inactivation, and 30 μM *trans*-Razo nearly completely activated thrombin. Hence, thrombin is active in the

DOI: 10.1021/jacs.5b11532
J. Am. Chem. Soc. 2016, 138, 955−961

trans-EIR system. This finding constitutes the second step toward our goal.

On the basis of our previous study,[47] UV-light treatment can promote the conversion of *trans*-Razo to *cis*-Razo, which exhibits a low binding affinity to DNA. We expected this process to trigger the unfolding of telomere DNA and to allow the 15Apt and 29Apt rebind together to the thrombin (Figure S5). Thrombin will consequently be switched to the "off" state. To test this hypothesis, we examined the effects of increasing durations of 365 nm UV illumination on the above *trans*-EIR system. The results demonstrate that more than half of the thrombin was inhibited after 20 s of 365 nm UV exposure and that a 60-s UV treatment completely inhibited thrombin (representative data in Figure 3). Thus, thrombin is inhibited in

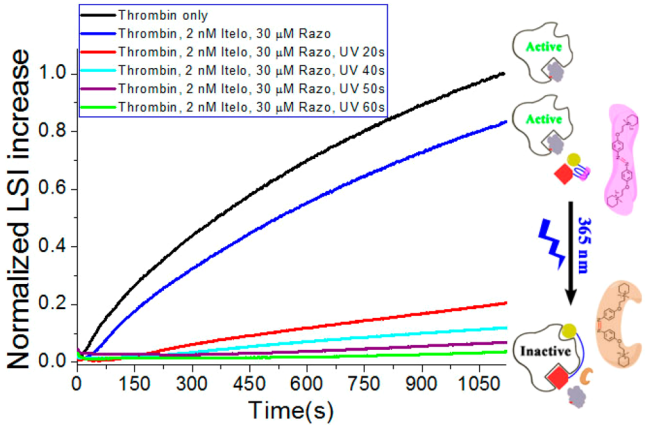

Figure 3. Inactivation efficacy under UV treatment of the *trans*-EIR system. Human thrombin (0.10 U/mL) was treated with the inhibitor Itelo (2.0 nM) and Razo (30 μM) and then irradiated with various durations of 365 nm UV light. The LSI increase of the sample was normalized to that of the control sample (thrombin only).

the *cis*-EIR system, which was generated by the *trans* to *cis* isomerization of Razo and the unfolding of telomere DNA under 365 nm UV. These findings constitute the third and key step toward our attempts at reversible regulation.

VIS (>400 nm) has been shown to be able to trigger the isomerization of *cis*-Razo to *trans*-Razo, which can compact and bind to telomere DNA.[47] The conformational changes of the regulatory domain will bring the 15Apt and 29Apt into close proximity and destroy their cooperative binding to thrombin, which will consequently be switched back to the "on" state (Figure S6). Our strategic direction is fully supported by the following results. As shown in Figure 4, a 20-s VIS treatment of the *cis*-EIR system evidently recovers thrombin activity, and this recovery is almost complete after 90 s of VIS illumination. Hence, thrombin was reactivated in the regenerated *trans*-EIR system, which was generated through the *cis* to *trans* isomerization of Razo, as well as the compacting of telomere DNA under VIS.

At this stage, thrombin had been successfully regulated after irradiation with one cycle of alternate UV and VIS (representative data in Figure 5A). Although it has been reported that *cis*-Razo cannot completely reisomerize to its *trans* form,[47] we observed similar enzyme activity between *trans*-Razo treated sample and VIS treated one (blue and purple lines in Figure 5A). The reason for this phenomenon could be that a large excess of Razo over Itelo was used to regulate thrombin activity. We further investigated the ability of this EIR

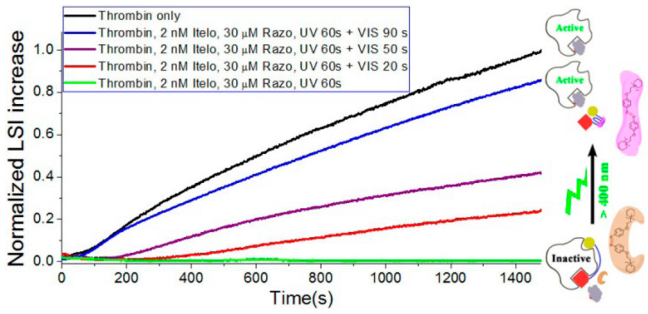

Figure 4. Reactivation efficacy under VIS treatment of the *cis*-EIR system. The solution containing human thrombin (0.10 U/mL), the inhibitor Itelo (2.0 nM) and Razo (30 μM) was exposed to 365 nm UV light (60 s) and then irradiated with various durations of VIS (>400 nm). The LSI increase of the sample was normalized to that of the control sample (thrombin without any treatment).

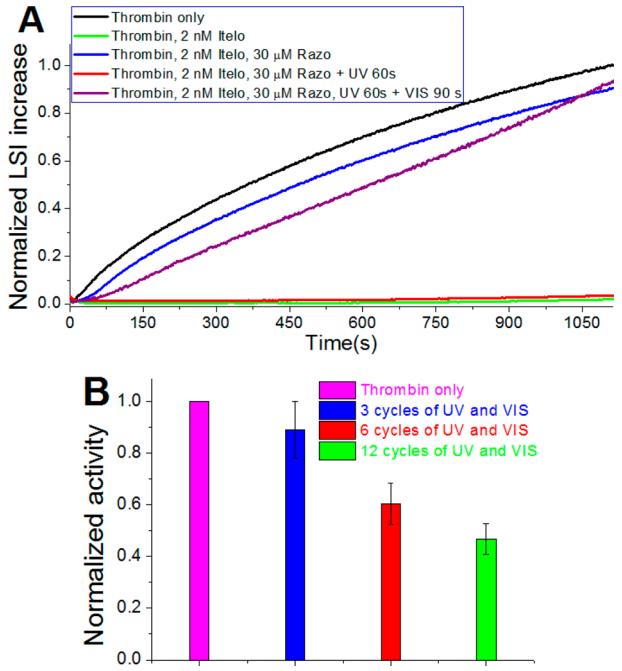

Figure 5. Photoregulation of the thrombin activities. (A) The LSI of the sample versus time is shown. The LSI increase of the sample was normalized to that of the control sample (untreated thrombin). The irradiation times with UV and VIS were 60 and 90 s, respectively. (B) Reversible regulation of thrombin upon multiple cycles of photo-irradiation.

system to retain reversible and repetitive photoregulation after multiple cycles of alternate UV and VIS. To this end, EIR samples were prepared according to the above protocol and further treated with alternating UV and VIS in parallel. One EIR sample per time was taken and assessed after the illumination step. The results consistently show that activities were negligible in all UV treated samples, whereas the activity of thrombin after 6 cycles of UV and VIS illumination was comparable with that of untreated thrombin (Figure 5B). The reversible regulation can be repeated 12 times without causing a significant loss of activity. Therefore, this test clearly indicates the good photoreversibility of our EIR system.

To elucidate the regulating mechanism, we then studied the ability of the typical G4 ligand TMPyP4[51] (left structure in Figure S7) to activate the above preinactive complex between

DOI: 10.1021/jacs.5b11532
J. Am. Chem. Soc. 2016, 138, 955−961

thrombin and Itelo. As expected, the thrombin activity recovered in the presence of 15 μM TMPyP4 (purple curve in Figure S8). A further assay indicated that TMPyP4 did not directly enhance the activities of thrombin in the absence of Itelo (Figure S9). To validate the G4-mediated action, further control assays were conducted. TMPyP2 (right structure in Figure S7) possesses a very similar structure to TMPyP4 but lacks the ability to stabilize and bind to G4 structures.[52] Therefore, it was used in our study. On the basis of the results, TMPyP2 treatment negligibly recovered thrombin activity compared with TMPyP4 (also Razo) at the same concentration (red curve in Figure S8). This significant difference between these two isomers suggested that a G4-mediated mechanism was involved in this process.

To further confirm that the telomere motif is targeted by Razo, multiple G-A mutations were introduced in this region to generate Itelo-Mut (sequence in Table S1). As shown in Figure S10A, this G4-mutated inhibitor also effectively inhibited thrombin activity (green curve), while Razo (15 μM) treatment did not markedly recover thrombin activity (blue curve). By contrast, the same concentration of Razo consistently recovered a much larger proportion of thrombin (blue curve in Figure S10B). These results suggest that Itelo-Mut did not undergo switched folding after Razo treatment.

Structural Switch of Itelo upon Photoirradiation of Razo. On the basis of the above activity assay, the flexible telomere fragment may act as a switch that controls thrombin. This process was then further structurally investigated. CD spectroscopy is a reliable and noninvasive method that can provide real-time information about the secondary structure adopted by DNA.[53] Figure 6A shows the overlaid CD spectra of Itelo in the absence or presence of Razo. The CD profile of Itelo (green line) reveals a typical hybrid G4 with a major positive band at approximately 290 nm (referred as band A), a shoulder band at approximately 260 nm (band B) and a negative band near 240 nm (band C).[54] Evidently, *trans*-Razo (30 μM) treatment shifted band B toward the longer wavelength region (red line). More importantly, a key difference was observed between the shapes of these two spectra. The maximum amplitude of band B was lower than that of band A for untreated Itelo (green line in Figure 6A), whereas a significantly opposing trend was observed after *trans*-Razo treatment (red line in Figure 6A). Because a 266 nm CD band is often associated with parallel-stranded G4,[53] *trans*-Razo binding markedly induced conformational changes in Itelo. We then examined the ability of the light-driven photoisomerization of Razo to induce structural changes in Itelo. Irradiation with 365 nm UV light for 1 min significantly reduced the height of band B, and the shape of the observed spectrum (black line in Figure 6A) was almost exactly the same as that of untreated Itelo. This result indicates that *cis*-Razo does not directly affect the secondary structure of Itelo due to low DNA binding ability. When the above sample was further irradiated with VIS for 90 s, an evident increase in band B was observed (blue line in Figure 6A), indicating the reversal of the Itelo conformation. In addition, the thermal melting curve of *trans*-Razo binding to Itelo was determined using CD at 266 nm. As shown in Figure S11, the unfolding process could not be accomplished at a high temperature, such as 90 °C, which further suggested that *trans*-Razo tightly bound to Itelo.

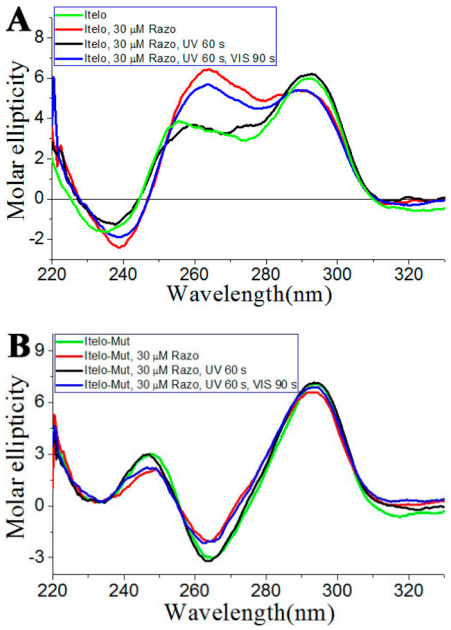

Figure 6. Representative CD spectra of Itelo or Itelo-Mut prior to and after photoirradiation of Razo are shown. The irradiation times with UV and VIS were 60 and 90 s, respectively. (A) Reversible compaction and extension of Itelo upon photoirradiation of Razo; (B) the spectrum of Itelo-Mut in the sample was only slightly altered upon photoirradiation of Razo.

To further confirm that the above observed effects originate from the telomere region, we also measured the CD profile of Itelo-Mut. The structure of this G4-mutated inhibitor was identified as a typical antiparallel G4 structure, with a dominant-positive peak at approximately 290 nm and a negative band at approximately 260 nm (green line in Figure 6B). Moreover, the CD profile of the sample after *trans*-Razo (30 μM) treatment was very similar to that of the starting Itelo-Mut, indicating that its structure remained almost unchanged (red line in Figure 6B). Not surprisingly, successive UV and VIS exposures did not significantly alter its CD spectra (black and blue lines in Figure 6B). Taken together, these results indicate that Razo can significantly affect the structure of Itelo because of its role in the reversible photocontrol of telomere conformation. Furthermore, Razo can modulate the activities of the preinactive complex between thrombin and Itelo.

Fluorescence Confocal Study of the Light-Regulating Process. Next, fluorescence confocal scanning laser microscopy (FCSLM) was used to study the reaction dynamics and further demonstrate our strategy. Here, Alexa Fluor 488-labeled fibrinogen was used as the substrate. When fluorescent fibrinogen was treated with thrombin (first row in Figure S12), the FCSLM image shows pieces of individual fibrin fibers and small fragments at t = 1 min (the leftmost column of image). As the reaction progressed, fibers rapidly aggregated into larger and more heterogeneous fibrins, which is an important characteristic of fibrinogenesis (the second to rightmost columns of image). When thrombin was treated with Itelo (second row in Figure S12), only small fragments of fiber was observed and almost no morphological and fluorescence changes occurred between t = 1 min (the leftmost column of image) and t = 60 min (the rightmost column of image). Therefore, Itelo completely stopped the aggregation of fibrin oligomers. When fibrinogen was treated with the *trans*-EIR system (first row in Figure 7), the fibrin oligomers aggregated at a rate comparable with that observed for

DOI: 10.1021/jacs.5b11532
J. Am. Chem. Soc. 2016, 138, 955−961

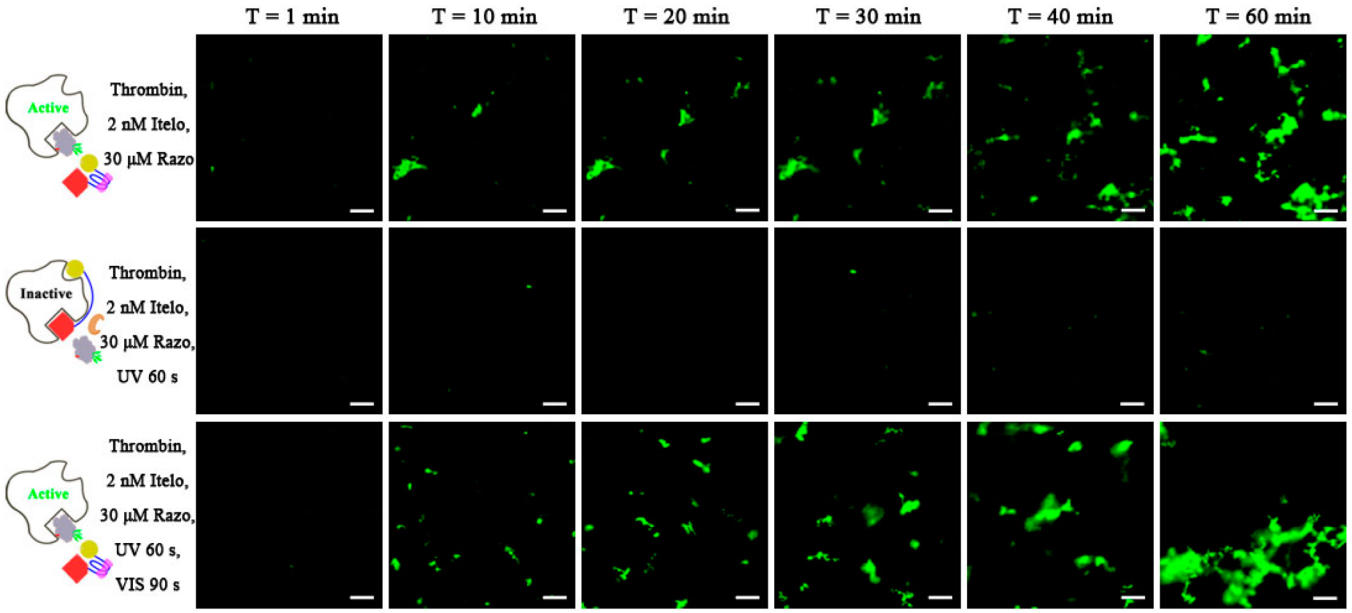

Figure 7. In situ examination of thrombin activity by FCSLM. Representative fluorescence images of the EIR sample are obtained at different time points (where $t = 0$ is the time of mixing of fluorescent fibrinogen and thrombin). All panels in the same row represent the same field of view (scale bar = 50 μm). The first row of images represents the initial *trans*-EIR system; the second row represents the *trans*-EIR system after 365 nm UV treatment (60 s); the third row represents the *trans*-EIR system after successive 365 nm UV (60 s) and VIS treatment (>400 nm, 90 s).

untreated thrombin and large fiber bundles appeared and spread over a larger area at $t = 10$ min (the second column of image). As a result, it was concluded that, thrombin activity recovered due to *trans*-Razo treatment. We then examined the effects of light exposure on the EIR system. The *trans*-EIR system was exposed to 365 nm UV light (1 min), followed by the addition of fluorescent fibrinogen. As shown in Figure 7 (second row in Figure 7), no morphological variation could be detected, even after a long time period ($t = 60$ min, the rightmost column of image), reflecting the complete inhibition of thrombin activity. When the above *trans*-EIR system was treated with a cycle of successive UV → VIS, it rapidly converted fibrinogen to fibrin (third row in Figure 7). Fibrin fibers began to be evident at $t = 10$ min (the second column of image), while fiber aggregates were larger and more numerous at $t = 20$ min (the third column of image), indicating that the thrombin activity had recovered. These FCSLM results therefore confirm the effectiveness of our light-controlled strategy, and the adjustment of light constitutes a convenient method to control thrombin.

Light-Regulating Blood Clotting of Human Plasma. Although our in vitro approach works well, controlling the enzyme activity in complex biological samples is more useful. We therefore tested the potency of our approach using human plasma samples. Thrombin-dependent blood clotting time (TCT) is a blood test that measures the time it takes for a clot to form in the plasma of a blood sample containing anticoagulant. In the current study, the TCT was determined and used as the parameter to judge the thrombin activity. Our results (Figure 8) demonstrate that the TCT of Itelo-treated samples (35.6 s) was much longer than that of untreated samples (15.6 s), reflecting the fact that Itelo is an effective inhibitor of blood plasma clotting. Strikingly, the averaged TCT (19.2 s) of Itelo/*trans*-Razo-treated plasma samples was similar to that of untreated samples, suggesting the efficient recovery of thrombin activity. More importantly, clotting is regulated by light-mediated Razo isomerization. After Itelo/*trans*-Razo-

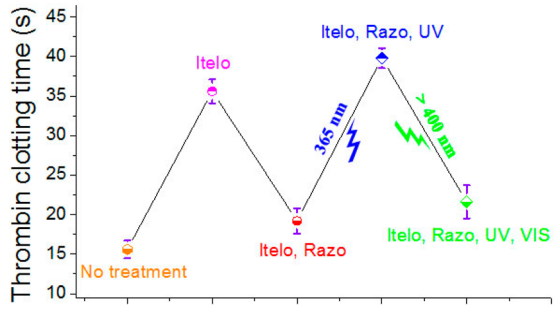

Figure 8. Clotting process of human plasma was regulated using our strategy. All data are presented as the means ± SEM from three independent experiments. The error bars reflect the standard deviation.

treated samples were exposed to 365 nm UV light for 1 min, the measured TCT was 39.8 s, indicating the inhibition of blood clotting. After the above samples were further exposed to VIS for 90 s, the averaged TCT value (21.6 s) was significantly decreased, suggesting a much faster clotting process. We believe that this success in regulating blood clotting further demonstrates the value of the newly developed strategy.

We expect that our strategy is general. In addition to the azobenzene derivative, our method also depends on a short oligonucleotide inhibitor that can bind to two adjacent sites on the target protein. To apply our strategy to control proteins other than thrombin, two binding partners that can cooperatively bind to their distinct binding sites on the target are required. These partners are then connected by telomere DNA to generate the photoresponsive inhibitor. Because the in vitro selection of aptamers against various protein targets has evolved into an automated process, such binding partners should be easily obtained.[55−57] The stability of Razo was examined in a cellular environment and the result revealed almost no destruction of this compound (Figure S13). Importantly, our MTT assay indicates that a high concentration

DOI: 10.1021/jacs.5b11532
J. Am. Chem. Soc. 2016, 138, 955−961

of Razo (125 μM) does not significantly reduce the viability of cultured HeLa cells (Figure S14). The micromolar concentrations of Razo needed to modulate thrombin activity are therefore low compared with the cytotoxic value of this molecule in vivo, indicating that our strategy may be used to control protein activity in cells using light in future applications.

CONCLUSION

In summary, we report the reversible photocontrol of enzymatic activity using a small molecule that functions through triggering the interconversion of telomere DNA between the compact and extended states. Compared with previous strategies, our approach is easy, cheap and surprisingly simple. Our strategy will therefore be potentially beneficial in future biomedical and pharmaceutical applications.

EXPERIMENTAL SECTION

Materials. Thrombin from human plasma (T6884), Fibrinogen from human plasma (F3879), Tris base (CAS# 77−86−1), KCl (CAS# 7447−40−7), Hydrochloric acid (CAS# 7647−01−0) and Thiazolyl Blue Tetrazolium Bromide (MTT, CAS# 298−93−1) were purchased from Sigma-Aldrich Inc. (St. Louis, MO, USA). Alexa Fluor 488 labeled fibrinogen (F13191) is purchased from Thermo Fisher Scientific Inc. (Waltham, MA, USA). 5,10,15,20-tetra-(*N*-methyl-2-pyridyl)porphine (TMPyP2) was purchased from Frontier Scientific (Logan, Utah, USA). The oligonucleotides were purchased from Invitrogen (Shanghai, China). The light scattering intensity (LSI) of the sample is determined using a LS55 fluorescence spectrometer (Perkin−Elmer Inc., USA) with the kinetics mode. The excitation and emission wavelengths were set at 650 and 650 nm, respectively. The detection is conducted at room temperature with a 1 cm path-length cell. CD experiments were performed on a Jasco-810 spectropolarimeter (Jasco, Easton, MD, USA) equipped with a Peltier temperature controller. The fluorescence confocal scanning laser microscopy (FCSLM) is performed using a laser scanning confocal microscope (Leica TCS SP2, Germany). Thrombin-dependent blood clotting time (TCT) was determined using an automatic ACL TOP 700 LAS hemostasis analyzer (Beckman Coulter Inc., Brea, CA).

Synthesis. Compounds Razo and TMPyP4 were synthesized according to previous literatures.[47,58]

Razo Activation Assay. Human thrombin was prepared as 0.10 U/mL in the reaction buffer (20 mM Tris-HCl at pH 7.4, 40 mM KCl) and the inhibitor Itelo (2.0 nM) was incubated in the thrombin solution for 15 min. The sample was then treated with various concentrations of Razo ranging from 0 μM to 30 μM for 15 min.

Light-Controlling Assay. For the light-controlling assay with 365 nm UV light, a portable UV analyzer (ZF-5, Shanghai Jia Peng Technology Co., Ltd.) was used. For the assay under VIS (>400 nm), a 50 W high-pressure mercury lamp was used as the light source, and a 400 nm long pass glass filter (model: LPF-400−01, Beijing Jinji Aomeng Co., Ltd.) was used to extract light of a longer wavelength than 400 nm. The sample was irradiated through an aperture at a distance of 3 cm by UV or VIS light.

Real-Time Monitoring of Thrombin Activity Using a Fluorescence Spectrometer. This assay was performed according to previous reports.[2,43] The curve describing LSI versus time was determined using the LS55 fluorescence spectrometer (Perkin−Elmer Inc., USA) with the kinetics mode at room temperature. The excitation and emission wavelengths are both set to 650 nm and a 1 cm path-length cell is used. Slit width: excitation = 10 nm; emission = 7 nm. For kinetic measurement, fibrinogen at a final concentration of 0.3 mg/mL was added at time (t) = 0. Thrombin without any treatment is used as an internal control. All of other samples were normalized to this standard.

Circular Dichroism Assay. CD experiments were performed using a Jasco-810 spectropolarimeter (Jasco, Easton, MD, USA) and a quartz cell (1 cm path length) at room temperature. CD spectra were determined from 200 to 340 nm at a scanning speed of 200 nm/min. The bandwidth was 5 nm and the response time was 2 s. All CD spectra were baseline-corrected for signal contributions due to the buffer and were the average of at least two runs.

Determination of Dynamic Morphological Changes of Fibrinogen. FCSLM is used to determine dynamic morphological changes of fluorescent fibrinogen catalyzed by thrombin. For this experiment, the sample is prepared as described above except that Alexa Fluor 488 labeled fibrinogen is used as the substrate. Then, immediately add one drop of each solution to the bottom of the small plastic Petri dish (35 mm) and carefully place a clean coverslip on the liquid drop. The Petri dish was then mounted and observed using a laser scanning confocal microscope (Leica TCS SP2, Germany). The laser used for excitation was 488 nm; the emission of green fluorescence was collected using the 505 to 530 nm band-pass filter. The images were recorded using a 40× oil objective, until no more morphological changes occur.

Blood Clotting Assays. This study was approved by the ethics committee of Zhongnan Hospital affiliated to Wuhan University. For research purposes, human blood samples were obtained from Zhongnan Hospital, and 333 μL of sodium citrate solution (0.109 M) was added to 3 mL of human blood from healthy volunteers. The mixture was subsequently centrifuged for 3 min at 3000 rpm at room temperature to remove blood cells, yielding plasma that was ready for analysis. The reaction solutions were prepared as described above. The TCTs of thrombin, Itelo-treated thrombin, Itelo-Razo-treated thrombin, Itelo-Razo-UV-treated thrombin or Itelo-Razo-UV−vis-treated thrombin solutions were determined using an automatic ACL TOP 700 LAS hemostasis analyzer (Beckman Coulter Inc., Brea, CA). The behavior of the scattering intensity was measured until the monitored signal reached a plateau. The TCT was defined as the time at which the velocity of clot formation was maximized.

Statistical Analysis. Statistical analysis was performed using the SPSS 19.0 software (SPSS Inc.). Differences were considered to be significant for $P < 0.05$.

ASSOCIATED CONTENT

Supporting Information

The Supporting Information is available free of charge on the ACS Publications website at DOI: 10.1021/jacs.5b11532.

General methods; sequences of the used oligomers; more experimental data and more experimental details. (PDF)

AUTHOR INFORMATION

Corresponding Authors

*xzhou@whu.edu.cn

*srwang@whu.edu.cn

Author Contributions

‡T.T. and Y.S. contributed equally.

Notes

The authors declare no competing financial interest.

ACKNOWLEDGMENTS

We thank the National Basic Research Program of China (973 Program) (2012CB720600, 2012CB720603, 2012CB720605), the National Science Foundation of China (No. 21432008, 91413109, 21372182, 21202126).

REFERENCES

(1) Zhou, C.; Yang, Z.; Liu, D. *J. Am. Chem. Soc.* **2012**, *134*, 1416.

(2) Kim, Y.; Phillips, J. A.; Liu, H.; Kang, H.; Tan, W. *Proc. Natl. Acad. Sci. U. S. A.* **2009**, *106*, 6489.

(3) Tzeng, S. R.; Kalodimos, C. G. *Nature* **2012**, *488*, 236.

(4) Laskowski, R. A.; Gerick, F.; Thornton, J. M. *FEBS Lett.* **2009**, *583*, 1692.

(5) Dagliyan, O.; Shirvanyants, D.; Karginov, A. V.; Ding, F.; Fee, L.; Chandrasekaran, S. N.; Freisinger, C. M.; Smolen, G. A.; Huttenlocher,

DOI: 10.1021/jacs.5b11532
J. Am. Chem. Soc. 2016, 138, 955−961

A.; Hahn, K. M.; Dokholyan, N. V. *Proc. Natl. Acad. Sci. U. S. A.* **2013**, *110*, 6800.
(6) Driver, J. A.; Zhou, X. Z.; Lu, K. P. *Discovery Med.* **2014**, *17*, 93.
(7) Arkin, M. R.; Wells, J. A. *Nat. Rev. Drug Discovery* **2004**, *3*, 301.
(8) Calamini, B.; Silva, M. C.; Madoux, F.; Hutt, D. M.; Khanna, S.; Chalfant, M. A.; Saldanha, S. A.; Hodder, P.; Tait, B. D.; Garza, D.; Balch, W. E.; Morimoto, R. I. *Nat. Chem. Biol.* **2012**, *8*, 185.
(9) Tasset, D. M.; Kubik, M. F.; Steiner, W. *J. Mol. Biol.* **1997**, *272*, 688.
(10) Bock, L. C.; Griffin, L. C.; Latham, J. A.; Vermaas, E. H.; Toole, J. J. *Nature* **1992**, *355*, 564.
(11) Pavlov, V.; Xiao, Y.; Shlyahovsky, B.; Willner, I. *J. Am. Chem. Soc.* **2004**, *126*, 11768.
(12) Liu, J.; Cao, Z.; Lu, Y. *Chem. Rev.* **2009**, *109*, 1948.
(13) Nutiu, R.; Li, Y. *J. Am. Chem. Soc.* **2003**, *125*, 4771.
(14) Li, D.; Song, S.; Fan, C. *Acc. Chem. Res.* **2010**, *43*, 631.
(15) Vinkenborg, J. L.; Karnowski, N.; Famulok, M. *Nat. Chem. Biol.* **2011**, *7*, 519.
(16) Wezenberg, S. J.; Chen, K. Y.; Feringa, B. L. *Angew. Chem., Int. Ed.* **2015**, *54*, 11457.
(17) Velema, W. A.; van der Berg, J. P.; Hansen, M. J.; Szymanski, W.; Driessen, A. J.; Feringa, B. L. *Nat. Chem.* **2013**, *5*, 924.
(18) Kasparkova, J.; Kostrhunova, H.; Novakova, O.; Krikavova, R.; Vanco, J.; Travnicek, Z.; Brabec, V. *Angew. Chem., Int. Ed.* **2015**, *54*, 14478.
(19) Yang, Y.; Goetzfried, M. A.; Hidaka, K.; You, M.; Tan, W.; Sugiyama, H.; Endo, M. *Nano Lett.* **2015**, *15*, 6672.
(20) Szymanski, W.; Beierle, J. M.; Kistemaker, H. A.; Velema, W. A.; Feringa, B. L. *Chem. Rev.* **2013**, *113*, 6114.
(21) Nishioka, H.; Liang, X.; Kato, T.; Asanuma, H. *Angew. Chem., Int. Ed.* **2012**, *51*, 1165.
(22) Crey-Desbiolles, C.; Lhomme, J.; Dumy, P.; Kotera, M. *J. Am. Chem. Soc.* **2004**, *126*, 9532.
(23) Jain, P. K.; Shah, S.; Friedman, S. H. *J. Am. Chem. Soc.* **2011**, *133*, 440.
(24) Shah, S.; Jain, P. K.; Kala, A.; Karunakaran, D.; Friedman, S. H. *Nucleic Acids Res.* **2009**, *37*, 4508.
(25) Heckel, A.; Mayer, G. *J. Am. Chem. Soc.* **2005**, *127*, 822.
(26) Hartley, G. *Nature* **1937**, *140*, 281.
(27) Griffiths, J. *Chem. Soc. Rev.* **1972**, *1*, 481.
(28) Yuan, Q.; Zhang, Y.; Chen, Y.; Wang, R.; Du, C.; Yasun, E.; Tan, W. *Proc. Natl. Acad. Sci. U. S. A.* **2011**, *108*, 9331.
(29) Stafforst, T.; Hilvert, D. *Angew. Chem., Int. Ed.* **2010**, *49*, 9998.
(30) Aemissegger, A.; Hilvert, D. *Nat. Protoc* **2007**, *2*, 161.
(31) Asanuma, H.; Liang, X.; Nishioka, H.; Matsunaga, D.; Liu, M.; Komiyama, M. *Nat. Protoc* **2007**, *2*, 203.
(32) Yamazawa, A.; Liang, X.; Asanuma, H.; Komiyama, M. *Angew. Chem., Int. Ed.* **2000**, *39*, 2356.
(33) Liang, X.; Wakuda, R.; Fujioka, K.; Asanuma, H. *FEBS J.* **2010**, *277*, 1551.
(34) Shao, Q.; Xing, B. *Chem. Soc. Rev.* **2010**, *39*, 2835.
(35) Liang, X.; Asanuma, H.; Komiyama, M. *J. Am. Chem. Soc.* **2002**, *124*, 1877.
(36) Asanuma, H.; Takarada, T.; Yoshida, T.; Tamaru, D.; Liang, X.; Komiyama, M. *Angew. Chem., Int. Ed.* **2001**, *40*, 2671.
(37) Brodin, J. D.; Auyeung, E.; Mirkin, C. A. *Proc. Natl. Acad. Sci. U. S. A.* **2015**, *112*, 4564.
(38) Lee, J. H.; Wong, N. Y.; Tan, L. H.; Wang, Z.; Lu, Y. *J. Am. Chem. Soc.* **2010**, *132*, 8906.
(39) Soderberg, O.; Gullberg, M.; Jarvius, M.; Ridderstrale, K.; Leuchowius, K. J.; Jarvius, J.; Wester, K.; Hydbring, P.; Bahram, F.; Larsson, L. G.; Landegren, U. *Nat. Methods* **2006**, *3*, 995.
(40) Flanigon, J.; Kamali-Moghaddam, M.; Burbulis, I.; Annink, C.; Steffen, M.; Oeth, P.; Brent, R.; van den Boom, D.; Landegren, U.; Cantor, C. *New Biotechnol.* **2013**, *30*, 153.
(41) Fredriksson, S.; Gullberg, M.; Jarvius, J.; Olsson, C.; Pietras, K.; Gustafsdottir, S. M.; Ostman, A.; Landegren, U. *Nat. Biotechnol.* **2002**, *20*, 473.
(42) Zhang, H.; Wang, Z.; Li, X. F.; Le, X. C. *Angew. Chem., Int. Ed.* **2006**, *45*, 1576.
(43) Wang, J.; Wei, Y.; Hu, X.; Fang, Y. Y.; Li, X.; Liu, J.; Wang, S.; Yuan, Q. *J. Am. Chem. Soc.* **2015**, *137*, 10576.
(44) Estevez-Torres, A.; Crozatier, C.; Diguet, A.; Hara, T.; Saito, H.; Yoshikawa, K.; Baigl, D. *Proc. Natl. Acad. Sci. U. S. A.* **2009**, *106*, 12219.
(45) Rajendran, A.; Endo, M.; Hidaka, K.; Sugiyama, H. *Angew. Chem., Int. Ed.* **2014**, *53*, 4107.
(46) Yangyuoru, P. M.; Di Antonio, M.; Ghimire, C.; Biffi, G.; Balasubramanian, S.; Mao, H. *Angew. Chem., Int. Ed.* **2015**, *54*, 910.
(47) Wang, X.; Huang, J.; Zhou, Y.; Yan, S.; Weng, X.; Wu, X.; Deng, M.; Zhou, X. *Angew. Chem., Int. Ed.* **2010**, *49*, 5305.
(48) Gosalia, D. N.; Salisbury, C. M.; Maly, D. J.; Ellman, J. A.; Diamond, S. L. *Proteomics* **2005**, *5*, 1292.
(49) Sambrano, G. R.; Weiss, E. J.; Zheng, Y. W.; Huang, W.; Coughlin, S. R. *Nature* **2001**, *413*, 74.
(50) Deng, B.; Lin, Y.; Wang, C.; Li, F.; Wang, Z.; Zhang, H.; Li, X. F.; Le, X. C. *Anal. Chim. Acta* **2014**, *837*, 1.
(51) Siddiqui-Jain, A.; Grand, C. L.; Bearss, D. J.; Hurley, L. H. *Proc. Natl. Acad. Sci. U. S. A.* **2002**, *99*, 11593.
(52) Han, H.; Langley, D. R.; Rangan, A.; Hurley, L. H. *J. Am. Chem. Soc.* **2001**, *123*, 8902.
(53) Karsisiotis, A. I.; Hessari, N. M.; Novellino, E.; Spada, G. P.; Randazzo, A.; Webba da Silva, M. *Angew. Chem., Int. Ed.* **2011**, *50*, 10645.
(54) Phan, A. T. *FEBS J.* **2010**, *277*, 1107.
(55) Liu, J.; You, M.; Pu, Y.; Liu, H.; Ye, M.; Tan, W. *Curr. Med. Chem.* **2011**, *18*, 4117.
(56) Cox, J. C.; Hayhurst, A.; Hesselberth, J.; Bayer, T. S.; Georgiou, G.; Ellington, A. D. *Nucleic Acids Res.* **2002**, *30*, e108.
(57) Nutiu, R.; Li, Y. *Angew. Chem., Int. Ed.* **2005**, *44*, 1061.
(58) Shi, D. F.; Wheelhouse, R. T.; Sun, D.; Hurley, L. H. *J. Med. Chem.* **2001**, *44*, 4509.

DOI: 10.1021/jacs.5b11532
J. Am. Chem. Soc. 2016, 138, 955−961